M. Valentini
Department of Mechanical and Structural Engineering, Faculty of Engineering, University of Trento, Via Mesiano 77, 38050 Povo, Trento, Italy

S. K. Serkov
Department of Mathematics, University of Utah, Salt Lake City, UT 84112

D. Bigoni
Department of Mechanical and Structural Engineering, Faculty of Engineering, University of Trento, Via Mesiano 77, 38050 Povo, Trento, Italy

A. B. Movchan[1]
Department of Mathematical Sciences, University of Liverpool, Liverpool L69 3BX, UK

Crack Propagation in a Brittle Elastic Material With Defects

A two-dimensional asymptotic solution is presented for determination of the trajectory of a crack propagating in a brittle-elastic, isotropic medium containing small defects. Brittleness of the material is characterized by the assumption of the pure Mode I propagation criterion. The defects are described by Pólya-Szegö matrices, and examples for small elliptical cavities and circular inclusions are given. The results of the asymptotic analysis, which agree well with existing numerical solutions, give qualitative description of crack trajectories observed in brittle materials with defects, such as porous ceramics.

1 Introduction

The analysis of failure mechanisms of brittle-composite materials has design implications in a broad range of contexts. These include defects—containing, porous, and particulate, or fiber-reinforced materials. Examples of these materials are: structural and traditional ceramics, which may contain flaws or pores, fibrous biological materials, porous rocks, porous high-strength metals at low temperature and ceramic or metal composites. In other materials, like concrete or certain rocks, stiff inclusions co-exist in a soft matrix with pores and microcracks. In this context, fracture propagation is the dominant failure mechanism at the microscale.

It is obvious that fracture propagation is affected by the presence of inhomogeneities, which modify the crack trajectory and, consequently, the toughness of the material. For instance, the toughening effect of a diluted porosity remains controversial (see, e.g., Claussen, (1976) and Duan et al. (1995) where the porosity consists of small cracks). In fact, on one hand, pores may act as stress concentrators and initiate strain localization and microcracking between cavities. On the other hand, pores may deviate the crack path from linearity and, when the crack tip intersects a cavity, this may produce a stress release. From the latter point of view, pores yield a shielding effect on crack propagation.

The above discussion elucidates the theoretical and practical relevance of developing analytical models capable of describing the fracture mechanisms of brittle materials containing voids or inclusions. This problem, numerically analyzed by Rubinstein (1986) and Rose (1986), is the focus of the present paper. In particular, an asymptotic solution is presented for the determination of the trajectory of a crack growing in an elastic-brittle isotropic material, under generalized plane conditions. With the term "brittle" we mean a material in which the fracture propagates according to the pure Mode I criterion or "criterion of local symmetry," i.e., $K_{II} = 0$ (Banichuk, 1970; Goldstein and Salganik, 1974). Two perturbed solutions are employed, one of which concerns the modification of the near-tip fields due to a perturbation from rectilinearity in the crack trajectory. In the other perturbed solution, defects are introduced and the modification on the near-tip field is evaluated. The former analysis is similar to some extent to that presented by Cotterell and Rice (1980). The latter analysis was initiated by Movchan, Nazarov, and Polyakova (1991) and is based on the concept of the Pólya-Szegö (1951) matrix, which characterizes the effect of the inclusion.

The model described in this article makes possible to investigate the effects of a number of inclusions on the trajectory of a crack. It is assumed that the characteristic size of defects is small compared to the distance from the crack trajectory and no interaction takes place between the defects. Examples are presented where defects are described by circular elastic inclusions and elliptical voids. Results are shown to agree with those presented by Rubinstein (1986) and are qualitatively consistent with crack patterns in brittle materials.

2 Problem Formulation

2.1 Crack Geometry and Field Equations. A quasi-static semi-infinite plane crack is considered, smoothly curved in the portion extending from the tip to a reference point where the crack profile becomes rectilinear, as indicated in Fig. 1. With respect to a coordinate system having the origin in the reference point and the axis x_1 tangent to the rectilinear crack profile, the crack tip has abscissa l. If the curved portion of the crack is sufficiently regular and close to rectilinearity, it can be

[1] To whom correspondence should be addressed. e-mail: abm@liv.ac.uk.

Contributed by the Applied Mechanics Division of THE AMERICAN SOCIETY OF MECHANICAL ENGINEERS for publication in the ASME JOURNAL OF APPLIED MECHANICS.

Discussion on the paper should be addressed to the Technical Editor, Professor Lewis T. Wheeler, Department of Mechanical Engineering, University of Houston, Houston, TX 77204-4792, and will be accepted until four months after final publication of the paper itself in the ASME JOURNAL OF APPLIED MECHANICS.

Manuscript received by the ASME Applied Mechanics Division, July 29, 1996; final revision, Aug. 3, 1998. Associate Technical Editor: J. L. Bassani.

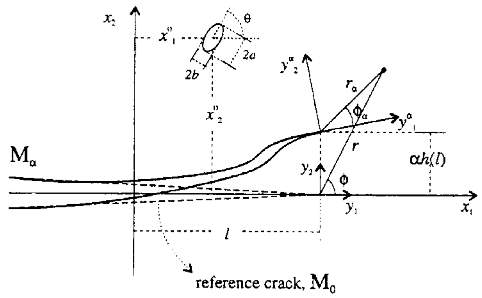

Fig. 1 Crack geometry

treated as *a perturbed straight crack*. In this case, the crack geometry can be specified by introducing a smooth function h of x_1, which, multiplied by a perturbation parameter α, specifies the x_2-coordinate of the curved portion of the crack. Therefore, the semi-infinite crack is described by the set $M_\alpha(l) := \{(x_1, x_2)\colon x_1 < l,\ x_2 = \alpha h(x_1)\}$, with $0 < \alpha \ll 1$. A defect is considered in the form of a cavity or an elastic inclusion, and is indicated by Ω_ϵ. The position of the defect is to some extent arbitrary, in the sense that it can be placed in an arbitrary point, but the ratio between the diameter of the defect and the minimal distance from crack trajectory has to be small enough to allow the use of a perturbation technique, that will be clarified in the following. It is therefore assumed that $\epsilon = \frac{1}{2}\,\mathrm{diam}\,\Omega_\epsilon/\mathrm{dist}\,(\Omega_\epsilon, M_\alpha) \ll 1$.

The crack problem regards plane strain (or stress) deformation of linear elastic, isotropic materials, characterized by the Lamé constants λ, μ, for the matrix material, and λ_0, μ_0, for the inclusion.

Vectors $\mathbf{u}$ and $\mathbf{u}^{(0)}$, representing the displacement fields in the matrix and inside the defect, respectively, are required to satisfy the Lamé equations

$$\mathbf{L}\mathbf{u} := \mu\Delta\mathbf{u} + (\lambda + \mu)\nabla\nabla\cdot\mathbf{u} = \mathbf{0},\qquad \mathbf{x} \in \mathbf{R}^2\backslash(\Omega_\epsilon \cup M_\alpha), \quad (1)$$

$$\mathbf{L}^{(0)}\mathbf{u}^{(0)} := \mu_0\Delta\mathbf{u}^{(0)} + (\lambda_0 + \mu_0)\nabla\nabla\cdot\mathbf{u}^{(0)} = \mathbf{0},\qquad \mathbf{x} \in \Omega_\epsilon, \quad (2)$$

and the boundary conditions. These consist of the traction-free condition at the crack faces

$$\boldsymbol{\sigma}^{(\mathbf{n})}(\mathbf{u}; \mathbf{x}) = \mathbf{0}, \quad \mathbf{x} \in M_\alpha^{\pm}, \quad (3)$$

(where $\boldsymbol{\sigma}^{(\mathbf{n})}$ is the stress vector relative to the elementary area of unit normal $\mathbf{n}$) and of two interface conditions at the inclusion boundary

$$\boldsymbol{\sigma}^{(\mathbf{n})}(\mathbf{u}; \mathbf{x}) = \boldsymbol{\sigma}^{(\mathbf{n},0)}(\mathbf{u}^{(0)}; \mathbf{x}), \quad \mathbf{u} = \mathbf{u}^{(0)}, \quad \mathbf{x} \in \partial\Omega_\epsilon. \quad (4)$$

In the case of a cavity, conditions (4) are replaced by the traction boundary condition

$$\boldsymbol{\sigma}^{(\mathbf{n})}(\mathbf{u}; \mathbf{x}) = \mathbf{0}, \quad \mathbf{x} \in \partial\Omega_\epsilon. \quad (5)$$

When the distance r from the crack tip tends to infinite, the displacement field is supposed to have the following asymptotic form:

$$\mathbf{u}(\mathbf{x}) \sim K_I^\infty r^{1/2}\boldsymbol{\Phi}^I(\phi), \quad \text{as} \quad r \to \infty, \quad (6)$$

where the stress intensity factor K_I^∞ is given, and the polar components of the vector function $\boldsymbol{\Phi}^I = (\Phi_r^I, \Phi_\phi^I)^t$ are specified by

$$\Phi_r^I(\phi) = \frac{1}{4\mu\sqrt{2\pi}}\left[(2\kappa - 1)\cos\frac{\phi}{2} - \cos\frac{3\phi}{2}\right],$$

$$\Phi_\phi^I(\phi) = \frac{1}{4\mu\sqrt{2\pi}}\left[\sin\frac{3\phi}{2} - (2\kappa + 1)\sin\frac{\phi}{2}\right], \quad (7)$$

where $\kappa = (\lambda + 3\mu)(\lambda + \mu)^{-1}$ for plane strain and $\kappa = (5\lambda + 6\mu)(3\lambda + 2\mu)^{-1}$ for plane stress.

2.2 Unperturbed Crack. The perturbation introduced by a defect on the near-tip crack fields is considered for a rectilinear crack M_0 (note that $\alpha = 0$ has been considered). For this problem, following Movchan et al. (1991) and Movchan and Movchan (1995) the displacement field *near the crack tip* can be represented as

$$\mathbf{u}(\mathbf{x}) \sim \mathbf{v}(\mathbf{x}) + \epsilon^2\mathbf{w}(\mathbf{x}), \quad (8)$$

where $\mathbf{v}(\mathbf{x}) = K_I r^{1/2}\boldsymbol{\Phi}^I(\phi)$ is the displacement field corresponding to a rectilinear crack in a plane without inclusion, and $\epsilon^2\mathbf{w}$ represents the correction term associated with the perturbation field produced by the small defect Ω_ϵ. The reason why the corrective term is second order in ϵ can be appreciated by considering the Neumann boundary value problem of a homogeneous elastic isotropic solid containing a defect (Movchan and Movchan, 1995, Section 1.3). The vector field $\mathbf{w}$ satisfies

$$\mathbf{L}\mathbf{w}(\mathbf{x}) = -\sum_{j,k=1}^{3}[(\mathbf{V}^{(j)}_{(\partial/\partial\mathbf{x})})^t\mathbf{v}(\mathbf{x})]_{\mathbf{x}=\mathbf{x}^0}\mathcal{P}_{jk}\mathbf{V}^{(k)}_{(\partial/\partial\mathbf{x})}\delta(\mathbf{x} - \mathbf{x}^0),\qquad \mathbf{x} \in R^2\backslash M_0, \quad (9)$$

(where $\mathbf{x}^0$ is the centre of the defect, and δ the Dirac function) and the homogeneous traction boundary conditions on the crack faces

$$\boldsymbol{\sigma}^{(\mathbf{n})}(\mathbf{w}; \mathbf{x}) = \mathbf{0}, \quad \mathbf{x} \in M_0^{\pm}. \quad (10)$$

In Eq. (9) $\mathcal{P}_{jk}$ are components of the Pólya-Szegö matrix of the defect and vectors $\mathbf{V}^{(j)}_{(\partial/\partial\mathbf{x})}$ are defined as

$$\mathbf{V}^{(1)}_{(\partial/\partial\mathbf{x})} := \begin{pmatrix} \dfrac{\partial}{\partial x_1} \\ 0 \end{pmatrix}, \quad \mathbf{V}^{(2)}_{(\partial/\partial\mathbf{x})} := \begin{pmatrix} 0 \\ \dfrac{\partial}{\partial x_2} \end{pmatrix},$$

$$\mathbf{V}^{(3)}_{(\partial/\partial\mathbf{x})} := \frac{1}{\sqrt{2}}\begin{pmatrix} \dfrac{\partial}{\partial x_2} \\ \dfrac{\partial}{\partial x_1} \end{pmatrix}. \quad (11)$$

Detailed discussion related to the structure of the matrix $\mathcal{P}$ will be given in Section 3.

2.3 Perturbation of the Crack Trajectory. We are now in a position to investigate the main problem, namely, perturbation of the crack trajectory induced by the presence of a defect. In the absence of defects, the crack would propagate rectilinearly under Mode I loading, a condition which trivially satisfies the criterion $K_{II} = 0$. The presence of a defect, even small, produces a perturbation in terms of a smooth deflection from linearity of crack trajectory.

Let us consider the asymptotic expansion of the displacement field near the tip of perturbed crack M_α. A local system of coordinates $\mathbf{y}^\alpha$ can be introduced, which has the origin centered in the tip of the perturbed crack (i.e., in the point of coordinates $(l, \alpha h(l))$) and axis y_1^α tangent to the crack trajectory at the crack tip (Fig. 1):

$$\mathbf{y}^{\alpha} = \begin{pmatrix} 1 & \alpha h'(l) \\ -\alpha h'(l) & 1 \end{pmatrix} \mathbf{y} - \begin{pmatrix} 0 \\ \alpha h(l) \end{pmatrix}, \quad (12)$$

where $\mathbf{y}$ is a system of coordinates translated with respect to $\mathbf{x}$, in particular, $\mathbf{y} = (y_1, y_2) = (x_1 - l, x_2)$.

In the polar coordinate system $\mathbf{y}^{\alpha}$ (Fig. 1), the asymptotic expansion of the displacement vector $\mathbf{u}$, relative to the perturbed crack, can be represented as follows:

$$\mathbf{u}(\mathbf{y}^{\alpha}) \sim \sum_{j=I,II} r_{\alpha}^{1/2} K_j(\alpha) \mathbf{\Phi}^{(j)}(\phi_{\alpha}),$$

$$K_j(\alpha) \sim K_j(l) + \alpha K_j'(l), \quad (13)$$

where quantities evaluated in l are referred to the unperturbed problem, so that $K_{II}(l) = 0$ by definition.

Moreover, displacement $\mathbf{u}(\mathbf{y}^{\alpha})$ may be represented in the system $\mathbf{y}$ through a rotation, i.e.,

$$\mathbf{u}(\mathbf{y}, \alpha) = \begin{pmatrix} 1 & -\alpha h'(l) \\ \alpha h'(l) & 1 \end{pmatrix} \mathbf{u}(\mathbf{y}^{\alpha}), \quad (14)$$

and, a Taylor series expansion of (14) can be performed near $\alpha = 0$:

$$\mathbf{u}(\mathbf{y}, \alpha) = \mathbf{u}(\mathbf{y}, 0) + \alpha \left.\frac{\partial \mathbf{u}(\mathbf{y}, \alpha)}{\partial \alpha}\right|_{\alpha=0} + O(\alpha^2). \quad (15)$$

Therefore, using Eqs. (13), (14), Eq. (15) becomes

$$\mathbf{u}(\mathbf{y}, \alpha) = \mathbf{u}(\mathbf{y}, 0) + \alpha \left\{ \begin{pmatrix} 0 & -h'(l) \\ h'(l) & 0 \end{pmatrix} \mathbf{v}(\mathbf{y}) + \left.\frac{\partial \mathbf{u}}{\partial y_1^{\alpha}} \frac{\partial y_1^{\alpha}}{\partial \alpha}\right|_{\alpha=0} + \left.\frac{\partial \mathbf{u}}{\partial y_2^{\alpha}} \frac{\partial y_2^{\alpha}}{\partial \alpha}\right|_{\alpha=0} + \left.\frac{\partial \mathbf{u}}{\partial K_I(\alpha)} \frac{\partial K_I(\alpha)}{\partial \alpha}\right|_{\alpha=0} + \left.\frac{\partial \mathbf{u}}{\partial K_{II}(\alpha)} \frac{\partial K_{II}(\alpha)}{\partial \alpha}\right|_{\alpha=0} \right\} + O(\alpha^2), \quad (16)$$

where $\mathbf{v}(\mathbf{y})$ is the same of Eq. (8).

The coefficient of the term multiplying α in Eq. (16) can be written as

$$\mathbf{u}'(\mathbf{y}) := -\frac{1+\kappa}{4\mu} h(l) K_I(l) r^{-1/2} \mathbf{\Psi}^{II}(\phi) + K_I'(l) r^{1/2} \mathbf{\Phi}^{I}(\phi) + \left[K_{II}'(l) - \frac{1}{2} K_I(l) h'(l) \right] r^{1/2} \mathbf{\Phi}^{II}(\phi), \quad (17)$$

where the components of the vector function $\mathbf{\Phi}^{I}$ are given by (7) and

$$\Phi_r^{II}(\phi) = \frac{1}{4\mu\sqrt{2\pi}} \left[(1 - 2\kappa) \sin\frac{\phi}{2} + 3 \sin\frac{3\phi}{2} \right],$$

$$\Phi_{\phi}^{II}(\phi) = \frac{1}{4\mu\sqrt{2\pi}} \left[3 \cos\frac{3\phi}{2} - (1 + 2\kappa) \cos\frac{\phi}{2} \right],$$

$$\Psi_r^{II}(\phi) = \frac{1}{\sqrt{8\pi}(1+\kappa)} \left[(1 + 2\kappa) \sin\frac{3\phi}{2} - \sin\frac{\phi}{2} \right],$$

$$\Psi_{\phi}^{II}(\phi) = \frac{1}{\sqrt{8\pi}(1+\kappa)} \left[(2\kappa - 1) \cos\frac{3\phi}{2} - \cos\frac{\phi}{2} \right]. \quad (18)$$

The stress components associated with (17) exhibit an unphysical strong singularity, and this fact indicates the presence of the boundary layer in the vicinity of the crack tip. This singularity may be eliminated in the way exposed in the following. First, let us introduce the weight function

$$\boldsymbol{\zeta}^{II}(\mathbf{y}) := r^{-1/2} \mathbf{\Psi}^{II}(\phi), \quad (19)$$

and therefore define

$$\mathbf{w}^*(\mathbf{y}) := \mathbf{u}'(\mathbf{y}) + \frac{1+\kappa}{4\mu} h(l) K_I(l) \boldsymbol{\zeta}^{II}(\mathbf{y}), \quad (20)$$

which satisfies the Lamé system (1) and the same boundary conditions on $M_0^{\mp}$ as $\mathbf{u}'$, but does not have a singularity at the crack tip $(l, 0)$.

Let us consider the ring $\Xi_R = \{\mathbf{y}: (1/R) \le \|\mathbf{y}\| \le R\}$, surrounding the reference crack tip, and the integral

$$\int_{\Xi_R/M_0} [\boldsymbol{\zeta}^{II}(\mathbf{y}) \cdot \mathbf{L}\mathbf{u}(\mathbf{y}) - \mathbf{u}(\mathbf{y}) \cdot \mathbf{L}\boldsymbol{\zeta}^{II}(\mathbf{y})] dy. \quad (21)$$

If the defect is far enough from the reference crack tip, representation (8) holds and therefore

$$\int_{\Xi_R \backslash M_0} [\boldsymbol{\zeta}^{II}(\mathbf{y}) \cdot \mathbf{L}\mathbf{u}(\mathbf{y}) - \mathbf{u}(\mathbf{y}) \cdot \mathbf{L}\boldsymbol{\zeta}^{II}(\mathbf{y})] dy = -\epsilon^2 \int_{\Xi_R \backslash M_0} [\boldsymbol{\zeta}^{II} \sum_{j,k=1}^{3} [(\mathbf{V}^{(j)}_{(\partial/\partial y)})^t \mathbf{v}]_{\mathbf{y}=\mathbf{y}^0} \mathcal{P}_{jk} \mathbf{V}^{(k)}_{(\partial/\partial y)}] \times \delta(\mathbf{y} - \mathbf{y}_0) dy = \epsilon^2 \sum_{j,k=1}^{3} \mathcal{P}_{jk} \mathcal{F}_{jk}(\mathbf{v}, \boldsymbol{\zeta}^{II}; \mathbf{y}^0), \quad (22)$$

where

$$\mathcal{F}_{jk}(\mathbf{v}, \boldsymbol{\zeta}^{II}; \mathbf{y}^0) := (\mathbf{V}^{(j)}_{(\partial/\partial y)})^t \mathbf{v}(\mathbf{y}^0) \mathbf{V}^{(k)}_{(\partial/\partial y)} \boldsymbol{\zeta}^{II}(\mathbf{y}^0). \quad (23)$$

If we reconsider integral (21), apply the Betti formula, and take the limit when R tends to infinity, we obtain

$$\lim_{R\to\infty} \int_{\Xi_R/M_0} [\boldsymbol{\zeta}^{II}(\mathbf{y}) \cdot \mathbf{L}\mathbf{u}(\mathbf{y}) - \mathbf{u}(\mathbf{y}) \cdot \mathbf{L}\boldsymbol{\zeta}^{II}(\mathbf{y})] dy$$

$$= \lim_{R\to\infty} \left\{ \int_{C_1} [\zeta_r^{II} \sigma_{rr}(\mathbf{u}) + \zeta_{\phi}^{II} \sigma_{r\phi}(\mathbf{u}) - u_r \sigma_{rr}(\boldsymbol{\zeta}^{II}) - u_{\phi} \sigma_{r\phi}(\boldsymbol{\zeta}^{II})] ds - \int_{C_2} [\zeta_r^{II} \sigma_{rr}(\mathbf{u}(\mathbf{y}, 0) + \alpha \mathbf{w}_r^*(\mathbf{y})) + \zeta_{\phi}^{II} \sigma_{r\phi}(\mathbf{u}(\mathbf{y}, 0) + \alpha \mathbf{w}_r^*(\mathbf{y})) - (u_r(\mathbf{y}, 0) + \alpha w_r^*(\mathbf{y})) \sigma_{rr}(\boldsymbol{\zeta}^{II}) - (u_{\phi}(\mathbf{y}, 0) + \alpha w_{\phi}^*(\mathbf{y})) \sigma_{r\phi}(\boldsymbol{\zeta}^{II})] ds + \sum_{\mp} \int_{M_0^{\mp}} [\zeta_1^{II} \sigma_{12}(\mathbf{u}) + \zeta_2^{II} \sigma_{22}(\mathbf{u}) - u_1 \sigma_{12}(\boldsymbol{\zeta}^{II}) - u_2 \sigma_{22}(\boldsymbol{\zeta}^{II})] ds \right\}$$

$$= 0 + \alpha\{\tfrac{1}{2} h'(l) K_I(l) - K_{II}'(l)\} + 0, \quad (24)$$

where $C_1(R) = \{\mathbf{y}: \|\mathbf{y}\| = R\}$ and $C_2 = \{\mathbf{y}: \|\mathbf{y}\| = 1/R\}$.

Note that in the integral along C_1, the field $\mathbf{u}$ corresponds to (6), whereas in the integral along C_2 the approximation (17), regularized via the weight function, is used. Finally, the integral along M_0 is null because of the traction free boundary conditions. Matching (24) with (22) it is concluded that $\alpha = \epsilon^2$, and the derivative of K_{II} is evaluated in the form

$$K_{II}'(l) = K_I(l) [\tfrac{1}{2} h'(l) - \sum_{j,k=1}^{3} \mathcal{P}_{jk} \mathcal{F}_{jk}(r^{-1/2} \mathbf{\Psi}^{II}, r^{1/2} \mathbf{\Phi}^{I}; \mathbf{y}^0)]. \quad (25)$$

Note that if the crack remains straight, i.e., if $h = 0$, relation (25) can be used to compare the present asymptotic solution to the numerical results of Rubinstein (1986) referred to the influence of defects on the near-tip fields of a rectilinear crack.

If the pure Mode I criterion of fracture is adopted, the orientation of the crack has to be chosen in such a way that $K_{II}(\alpha) = 0$, and therefore

$$K_{II}(\alpha) \sim \alpha K'_{II}(l) = 0, \tag{26}$$

which can be substituted into Eq. (25) to get

$$h'(l) = 2 \sum_{j,k=1}^{3} \mathcal{P}_{jk}\mathcal{F}_{jk}(r^{-1/2}\boldsymbol{\Psi}^{II}, r^{1/2}\boldsymbol{\Phi}^{I}; \mathbf{y}^0). \tag{27}$$

Equation (27) can be easily integrated[2] to obtain the solution for the crack deflection function in the case when the center of the inclusion is placed at the generic point (x_1^0, x_2^0):

$$h(l) = \frac{4\mu}{x_2^0(\kappa+1)}\{\cos\phi\mathcal{L}'(\phi)\mathcal{P}\mathcal{L}(\phi) - \mathcal{L}'(0)\mathcal{P}\mathcal{L}(0)\}, \tag{28}$$

where $\cos\phi = (x_1^0 - l)[(x_2^0)^2 + (x_1^0 - l)^2]^{-1/2}$, and[3]

$$\mathcal{L}(\phi) = \begin{pmatrix} \dfrac{1}{4\mu\sqrt{2\pi}}\cos\dfrac{\phi}{2}\left[\kappa - 1 - 2\sin\dfrac{\phi}{2}\sin\dfrac{3\phi}{2}\right] \\ \dfrac{1}{4\mu\sqrt{2\pi}}\cos\dfrac{\phi}{2}\left[\kappa - 1 + 2\sin\dfrac{\phi}{2}\sin\dfrac{3\phi}{2}\right] \\ \dfrac{1}{4\mu\sqrt{\pi}}\sin\phi\cos\dfrac{3\phi}{2} \end{pmatrix}. \tag{29}$$

$$\mathbf{T}(\mathbf{x}) = \frac{\lambda+\mu}{8\pi\mu(\lambda+2\mu)}\begin{pmatrix} -2\kappa\ln\sqrt{x_1^2+x_2^2} + \dfrac{2x_1^2}{x_1^2+x_2^2} & \dfrac{2x_1x_2}{x_1^2+x_2^2} \\ \dfrac{2x_1x_2}{x_1^2+x_2^2} & -2\kappa\ln\sqrt{x_1^2+x_2^2} + \dfrac{2x_2^2}{x_1^2+x_2^2} \end{pmatrix}. \tag{33}$$

It may be important to remark that the problem of the interaction of a crack with more than one defect can be solved in a straightforward way in the present framework, when it is assumed that defects do not interact. In particular, when a number of defects is considered, their effect consists in a modification of Eq. (8), where the sum of the perturbative terms relative to all defects replaces the single term $\epsilon^2\mathbf{w}$.

3 The Pólya-Szegö Matrices

The Pólya-Szegö matrix $\mathcal{P}$ characterizes the morphology of the inclusion and its elastic properties. The properties of the dipole tensors for boundary value problems related to the Laplacian were given by Pólya and Szegö (1951). For problems of elasticity, the dipole tensors were analyzed by Zorin et al. (1988), Babich et al. (1989), Movchan (1992), and Movchan and Serkov (1991). In this section we briefly discuss the definitions and give explicit representation for the dipole matrices corresponding to circular inclusions and elliptical cavities.

Definitions. Let us go back to the problem of an infinite plane with a finite inclusion or cavity Ω_ϵ, presented in Section 2.2. In that section, the unperturbed, i.e., without defect solution was identified with the solution corresponding to a static rectilinear crack in a plane. In the case of a plane with a defect, the solution can be represented as a linear combination of the vectors $\mathbf{U}^{(j)}$ $(j = 1, 2, 3)$, satisfying the homogeneous Lamé system and admitting the representation

$$\mathbf{U}^{(j)}(\mathbf{x}) = \mathbf{V}_{\mathbf{x}}^{(j)} + \mathbf{W}^{(j)}(\mathbf{x}), \tag{30}$$

where

$$\mathbf{V}_{\mathbf{x}}^{(1)} = (x_1, 0)^t, \quad \mathbf{V}_{\mathbf{x}}^{(2)} = (0, x_2)^t,$$

$$\mathbf{V}_{\mathbf{x}}^{(3)} = 2^{-1/2}(x_2, x_1)^t, \tag{31}$$

and the vector field $\mathbf{W}^{(j)}$, decaying at infinity, can be expressed as

$$\mathbf{W}^{(j)} = \sum_{k=1}^{3} \mathcal{P}_{jk}[\mathbf{V}_{(\partial/\partial\mathbf{x})}^{(k)}]^t\mathbf{T}(\mathbf{x}) + O(|\mathbf{x}|^{-2}). \tag{32}$$

Apart from factor ϵ^2 which is now included in $\mathcal{P}$, this matrix is the Polya-Szegö matrix defined in Section 2.2, whereas $\mathbf{T}$ is the Kelvin-Somigliana matrix (Fichera, 1972) defined as (33).

A Circular Inclusion. In the case of an elastic circular inclusion of radius R, having Lamé constants λ_0, μ_0, the outside-inclusion displacement field $\mathbf{u} = (u_1, u_2)$ can be represented, via complex Kolosov-Muskhelishvili (1953) potentials $\varphi(z)$ and $\psi(z)$, as

$$u_1 + iu_2 = (2\mu)^{-1}[\kappa\varphi(z) - z\overline{\varphi'(z)} - \overline{\psi(z)}], \tag{34}$$

where

$$\varphi(z) = \alpha z + \frac{\bar{\gamma}R^2}{z}\frac{\mu_0 - \mu}{\kappa\mu_0 + \mu},$$

$$\psi(z) = \gamma z + \frac{\mathrm{Re}\,(\alpha)R^2}{z}\frac{2\mu_0(\kappa-1) - 2\mu(\kappa_0 - 1)}{\mu(\kappa_0 - 1) + 2\mu_0} + \frac{\bar{\gamma}R^4}{z^3}\frac{\mu_0 - \mu}{\kappa\mu_0 + \mu}. \tag{35}$$

Constants α and γ in Eq. (35) can be determined from the conditions at infinity. In particular, when the displacement field behaves like $\mathbf{V}_{\mathbf{x}}^{(j)}$ + smaller terms, as $\|\mathbf{x}\| \to \infty$, it can be shown that

[2] The following auxiliary identity may be helpful in the integration

$$\zeta^{II} = \frac{4\mu}{\kappa+1}\frac{\partial(r^{1/2}\boldsymbol{\Phi}^I)}{\partial y_2}.$$

[3] It may be noted that Cartesian components of the vector $\mathcal{L}$ are given by

$$\mathcal{L}_k = r^{1/2}((\mathbf{V}_{(\partial/\partial\mathbf{y})}^{(k)})^t(r^{1/2}\boldsymbol{\Phi}^I(\phi)))_{\mathbf{y}=\mathbf{y}^0}.$$

$$\alpha = \frac{\mu}{\kappa - 1}, \quad \gamma = -\mu, \quad \text{for} \quad j = 1,$$

$$\alpha = \frac{\mu}{\kappa - 1}, \quad \gamma = \mu, \quad \text{for} \quad j = 2,$$

$$\alpha = 0, \quad \gamma = i\mu\sqrt{2}, \quad \text{for} \quad j = 3. \tag{36}$$

In addition to representation (34), the displacement field at infinity can be represented as a linear combination of vectors $\mathbf{U}^{(j)}$ (30), plus smaller terms. The asymptotic expression (32) for the field $\mathbf{W}^{(j)}$ can be rewritten via the complex variable $z = x_1 + ix_2$ in the form

$$W_1^{(j)} + iW_2^{(j)} = \mathcal{P}_{j1}\left(\frac{\partial}{\partial z}[T_{11} + iT_{12}] + \frac{\partial}{\partial \bar{z}}[T_{11} + iT_{12}]\right)$$

$$+ \mathcal{P}_{j2}\left(\frac{\partial}{\partial z}[-T_{22} + iT_{12}] + \left(\frac{\partial}{\partial \bar{z}}[T_{22} - iT_{12}]\right)\right.$$

$$+ \frac{1}{\sqrt{2}}\mathcal{P}_{j3}\left(\frac{\partial}{\partial z}[iT_{11} + iT_{22}]\right.$$

$$\left.+ \left(\frac{\partial}{\partial \bar{z}}[2T_{12} + i(T_{22} - T_{11})]\right)\right) + O\left(\frac{1}{|z|^2}\right), \tag{37}$$

where

$$\mathbf{T} = \frac{\lambda + \mu}{8\pi\mu(\lambda + 2\mu)}\begin{pmatrix} -2\kappa \ln|z| + \dfrac{z^2 + \bar{z}^2 + 2z\bar{z}}{2z\bar{z}} & \dfrac{z^2 - \bar{z}^2}{2iz\bar{z}} \\ \dfrac{z^2 - \bar{z}^2}{2iz\bar{z}} & -2\kappa \ln|z| - \dfrac{z^2 + \bar{z}^2 - 2z\bar{z}}{2z\bar{z}} \end{pmatrix}, \tag{38}$$

is the complex variable representation of the Kelvin-Somigliana matrix.

Comparing relations (34) and (37), it is concluded that the Pólya-Szegö matrix for the given elastic circular inclusion can be expressed in the form

$$\mathcal{P} = \frac{R^2}{4q}\begin{pmatrix} \Xi + \Theta & \Xi - \Theta & 0 \\ \Xi - \Theta & \Xi + \Theta & 0 \\ 0 & 0 & 2\Theta \end{pmatrix}, \tag{39}$$

where

$$q = \frac{\lambda + \mu}{8\pi\mu(\lambda + 2\mu)}, \quad \Theta = \frac{\mu_0 - \mu}{\kappa\mu_0 + \mu},$$

$$\Xi = \frac{1}{(\kappa - 1)^2}\frac{2\mu_0(\kappa - 1) - 2\mu(\kappa_0 - 1)}{\mu(\kappa_0 - 1) + 2\mu_0}. \tag{40}$$

An Elliptical Cavity. In the case of an elliptical cavity in an isotropic elastic plane, we denote with a and b the large and small semi-axes of ellipse, respectively, and with θ the angle between the x_1-axis and the largest axis of the ellipse. The conformal mapping of the exterior of the unit disk into the exterior of the elliptical cavity can be given as

$$\omega(\xi) = \frac{a + b}{2}\left(\xi + m\frac{e^{2i\theta}}{\xi}\right), \quad m = \frac{a - b}{a + b}, \tag{41}$$

and therefore, the solution $\mathbf{u}$, expressed via complex potentials, becomes

$$u_1 + iu_2 = (2\mu)^{-1}\left[\kappa\varphi(\xi) - \frac{\omega(\xi)}{\overline{\omega'(\xi)}}\overline{\varphi'(\xi)} - \overline{\psi(\xi)}\right]. \tag{42}$$

Taking into account the condition at infinity and the traction-free boundary condition at the cavity boundary, the Pólya-Szegö matrix can be obtained in the following form (Movchan[4], 1992):

$$\mathcal{P} = -\frac{1}{4\mu}(a + b)^2\pi(\lambda + 2\mu)$$

$$\times \begin{pmatrix} \Xi + \Theta + \Sigma & \Xi - \Theta & \Lambda \\ \Xi - \Theta & \Xi + \Theta - \Sigma & \Lambda \\ \Lambda & \Lambda & 2\Theta \end{pmatrix}, \tag{43}$$

where

$$\Theta = \frac{2\mu^2}{\lambda + \mu}, \quad \Xi = (\lambda + \mu)(1 + m^2),$$

$$\Sigma = -4\mu m \cos 2\theta, \quad \Lambda = -2\sqrt{2}\mu m \sin 2\theta. \tag{44}$$

4 Interaction Between a Semi-infinite Crack and a Cavity

As a first application of the presented theory, we consider the case of interaction of a semi-infinite crack and an elliptical cavity Ω_ϵ with the largest axis inclined at the angle θ to the x_1-axis. The center of the ellipse is located at (x_1^0, x_2^0). Substituting (43) into (28) we obtain

$$H(l) = \epsilon^2 h(l) = \frac{R^2}{2x_2^0}[2(1 + m^2) - z(2 + z - z^2$$

$$+ m^2(1 + z) + 2m\cos 2\theta(1 + 2z)(1 - z^2)$$

$$- 2m \sin 2\theta(2z - 1)(1 + z)\sqrt{1 - z^2})], \tag{45}$$

where

$$z = \frac{-l + x_1^0}{\sqrt{(x_2^0)^2 + (-l + x_1^0)^2}}, \quad R = \frac{a + b}{2}.$$

It should be noted that conditions $m = 0$ and $m = 1$ correspond to the relevant cases of a circular void and of a Griffith crack, respectively.

The crack trajectories $h(l)$, as obtained from (45), are reported in Fig. 2. In particular, the crack trajectory is plotted in Fig. 2(a) resulting from the interaction of a semi-infinite crack with an ellipse having the major axis parallel to x_1 and center at (0, 1). Different aspect ratio are investigated. Figure 2(b) pertains to the case of a semi-infinite crack interacting with a Griffith crack inclined at different angles.

It should be noted that in the case of a circular cavity, $m = 0$, $H(l)$ takes positive values for every l. Therefore, a circular cavity always "attracts" a crack. In the case of an elliptical void, the situation is more complicated. In fact the trajectory of the crack is influenced by the orientation of the ellipse and

[4] Note that in the formula analogous to (43) of the paper by Movchan (1992), the $\sqrt{2}$ factor was missed in the term Λ.

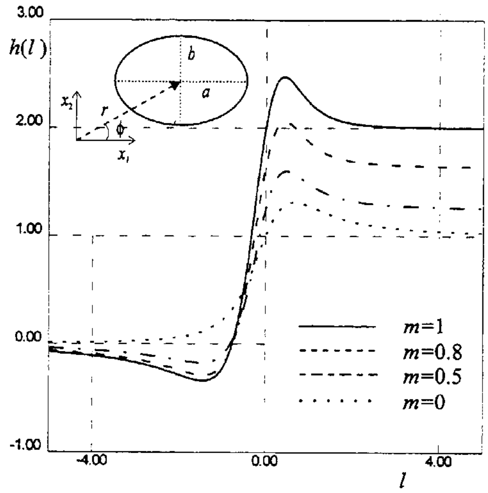

Fig. 2(a) Elliptic cavity, with major axis parallel to the main crack. Results reported for different aspect ratios.

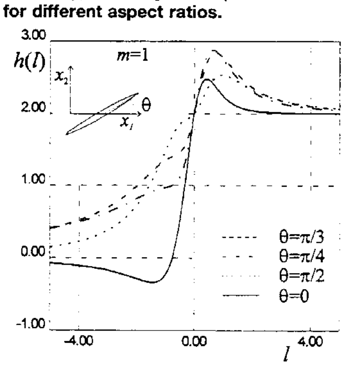

Fig. 2(b) Griffith crack at different inclinations

Fig. 2 Crack trajectory $h(l)$ versus crack-tip position l, resulting from interaction with a cavity

by the aspect ratio a/b. In particular, the crack may suffer a slight repulsion, followed by a strong attraction (so that curves relative to Fig. 2(a) have a minimum followed by a maximum). In any case, the deflection at infinity always corresponds to attraction. This can be verified by observing that the limit $l \to +\infty$ of (28)

$$H_\infty = -\frac{\epsilon^2 4\mu}{\kappa + 1}[\mathcal{L}(0)\mathcal{P}\mathcal{L}(0)] = \frac{R^2}{x_2^0}(1 + m^2), \quad (46)$$

is always positive, the dipole matrix $\mathcal{P}$ being negative definite for any cavity of finite dimension. Moreover, H_∞ increases when parameter m increases (Fig. 2(a)). This means that the deflection due to interaction with a thin ellipse is greater than the deflection produced by a circular cavity with diameter equal to the crack length.

Note from Fig. 2(b), that for any orientation of the Griffith crack, all crack trajectories intersect at the point corresponding to $l = 0$. Moreover, $H(0) = H_\infty$ and therefore the crack deflection at infinity is independent of the orientation of the small defect. However, the change of the angle θ affects the shape of the crack trajectory in the vicinity of the origin.

A SEM photograph is reported in Fig. 3(a) of a crack path induced by Vicker indenter in a sample of porcelain stoneware. This particular ceramic contains a dilute concentration of near-ellipsoidal voids. These voids have been modeled as ellipses in Fig. 3(b), where the crack trajectory has been obtained using the solution developed above. Obviously, certain approximations of the model may be anticipated. In particular, interactions between voids has been neglected; moreover, the assumption of small ratio between void dimension and distance from the crack tip is often forced. Perhaps more important, the model refers to a situation of plane strain, whereas the physical problem may be three-dimensional. However, we note from Fig. 3 that, in spite of all the approximations, the mathematical model gives an excellent description of the physical situation.

In closure of this section, a comparison is presented of the theory developed in this article to numerical solution of the singular integral equation for the complex crack opening given by Rubinstein (1986). To this purpose, $h'(l) = 0$ is considered in Eq. (25), which gives the the normalised Mode II stress intensity factor in the case when the unperturbed state corresponds to the Mode I load (characterized by the stress infinity factor K_I^∞)

$$K_{II}/K_I^\infty \sim \frac{R^2}{r^2}\sum_{j,k=1}^{3}\mathcal{P}_{jk}\mathcal{F}_{jk}(r, \phi), \quad (47)$$

with (r, ϕ) being polar coordinates of a small defect.

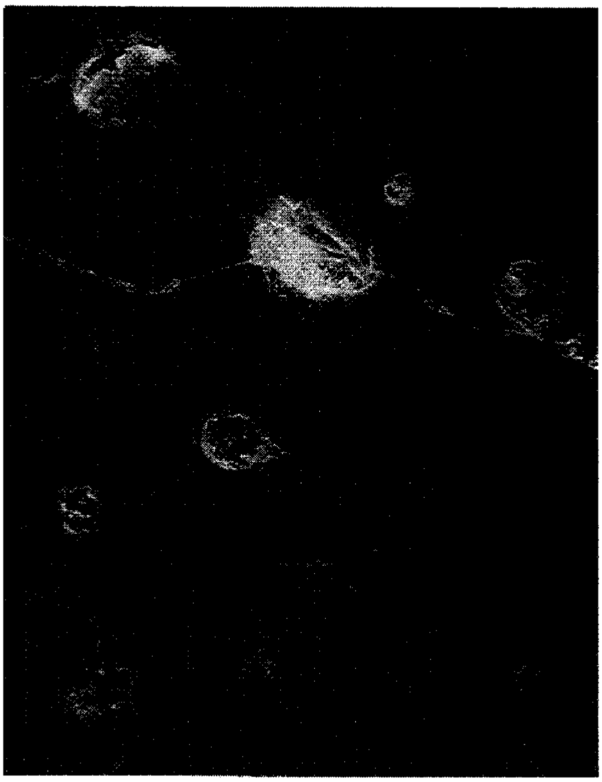

Fig. 3(a) SEM photograph of a crack in a porcelain stoneware

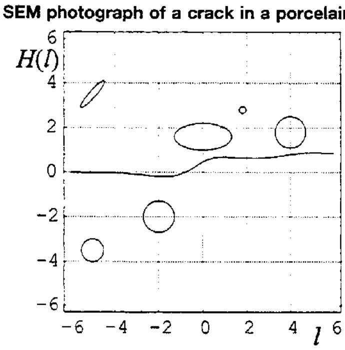

Fig. 3(b) Model prediction

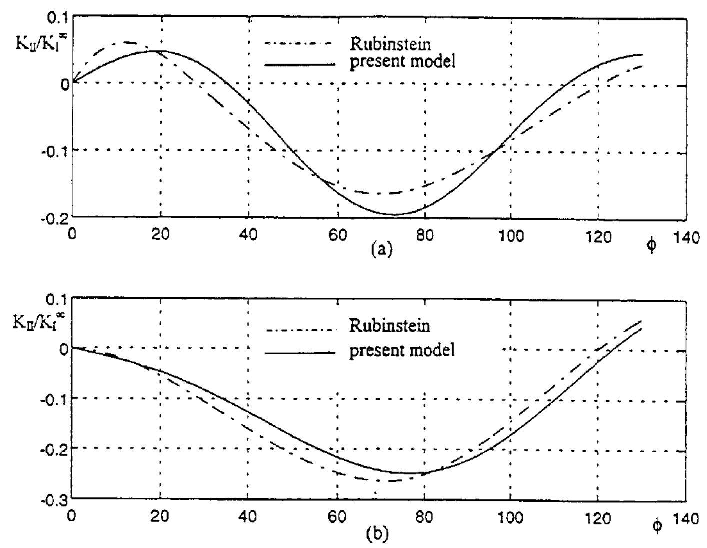

Fig. 4 Comparison with Rubinstein's results, Mode II normalized stress intensity factor versus defect position ϕ; (a) interaction with a Griffith crack, (b) interaction with a circular cavity

Comparison with Rubinstein's results is reported in Fig. 4(a) and (b), where the cases of a Griffith crack and a circular cavity are considered, respectively. Note that the Mode II normalised stress intensity factors are reported versus ϕ, the angle of orientation of the position vector relative to the small defect (Fig. 1). Obviously, since (47) is an approximate asymptotic formula, a discrepancy with the numerical results of Rubinstein can be expected. The error is however quite small and the results of explicit asymptotic analysis show the right qualitative behaviour of the stress intensity factor as a function of the angular variable ϕ.

5 Interaction Between a Semi-infinite Crack and a Circular Elastic Inclusion

In the case of a circular inclusion, the Pólya-Szegö matrix $\mathcal{P}$ is given by (39). Consequently, formula (28) gives

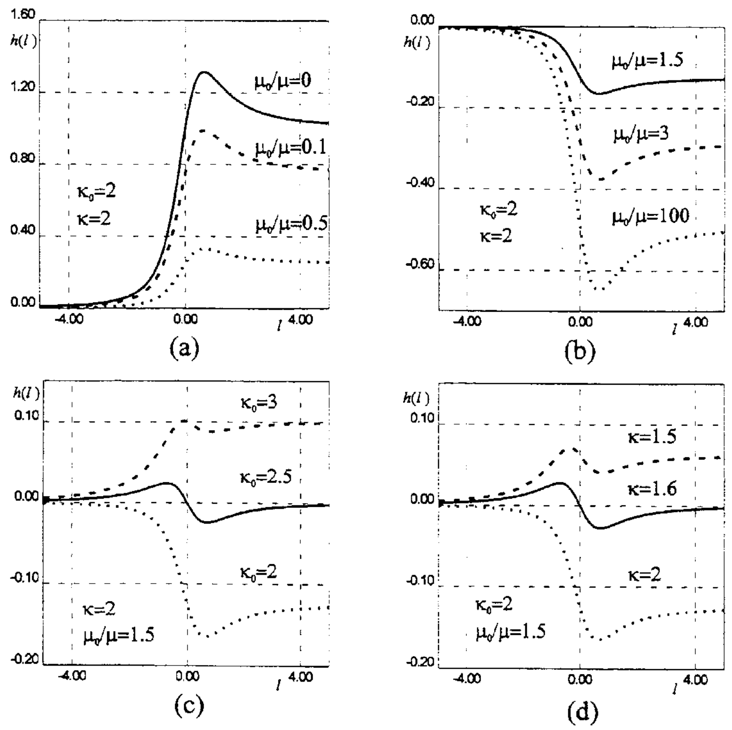

Fig. 5 Crack trajectory $h(l)$ versus crack-tip position l, resulting from interaction with an elastic circular inclusion; (a) inclusion more rigid than the matrix, (b) inclusion less rigid than the matrix, (c) and (d) cases in which $\mathcal{P}$ is indefinite.

$$H(l) = \epsilon^2 h(l)$$

$$= \frac{R^2}{2x_2^0}\left[(z^2 + z - 2)\frac{\mu_0(\kappa - 1) - \mu(\kappa_0 - 1)}{\mu(\kappa_0 - 1) + 2\mu_0} + (z - z^3)\frac{\mu_0 - \mu}{\kappa\mu_0 + \mu}\right], \quad (48)$$

where R is the radius of the inclusion and

$$z = \frac{-l + x_1^0}{\sqrt{(x_2^0)^2 + (-l + x_1^0)^2}}.$$

In the particular case when $\mu_0 = 0$, Eq. (48) reduces to Eq. (45) with $m = 0$, which corresponds to the case of a circular cavity. In plain strain, the Pólya-Szegö matrix $\mathcal{P}$ of a circular inclusion is positive definite when

$$\frac{\mu_0}{\mu} > 1 \quad \text{and} \quad \frac{\lambda_0 + \mu_0}{\lambda + \mu} > 1, \quad (49)$$

and is negative definite when the inequalities (49) are both reversed. Otherwise, the matrix $\mathcal{P}$ is indefinite.

The crack deflection at infinity is given by

$$H_\infty = \epsilon^2 h_\infty = \frac{R^2}{x_2^0}\left\{1 - \frac{\mu_0(\kappa + 1)}{2\mu_0 + (\kappa_0 - 1)\mu}\right\}. \quad (50)$$

Crack trajectories $h(l)$ relative to the interaction of a semi-infinite crack with an elastic circular inclusion centered at (0, 1) are reported in Fig. 5, for different values of elastic parameters. It can be noted that the defect tends to attract the crack in the case of an inclusion less rigid than the matrix (Fig. 5(*a*)), whereas in the opposite case of an inclusion more rigid than the matrix, the crack tends to be repelled by the defect (Fig. 5(*b*)). Figures 5(*c*) and (*d*) refer to cases in which matrix $\mathcal{P}$ is indefinite. Note in this case that a set of parameters can be chosen, for which the deflection at infinity is equal to zero.

6 Conclusions

Application of perturbative techniques to the problem of fracture propagation in an elastic material has been shown to be relevant in obtaining approximate solutions of interaction of a semi-infinite crack with defects.

Accepting the hypotheses of noninteracting defects and small ratio between defect diameter and distance to the crack, an analytical solution for the crack trajectory has been presented. This solution gives qualitative information on crack path in brittle materials. In particular, inclusions less rigid than the matrix generally "attract" the crack, whereas an opposite effect is observed in the case of inclusions more rigid than the matrix. In conclusion, a model has been presented to obtain the shape of crack trajectory as influenced by number, position, form, and elastic constants of the defects.

Acknowledgments

The authors would like to thank Prof. J.R. Willis (Cambridge University) for helpful discussions and Dr. A. Tucci and Dr. L. Esposito (Ceramic Centre, Bologna) for assistance with the experiment. M. V. acknowledges the financial support of the TMR European fund (Contr. ERBCHRXCT930383) and is grateful to Bath University (School of Mathematical Sciences) for provision of computing facilities. D. B. and M. V. acknowledge the financial support of Italian MURST 60%.

References

Babich, V.M., Zorin, I.S., Ivanov, M.I., Movchan, A.B., and Nazarov, S.A., 1989, "Integral characteristics in problems of elasticity," *Steklov Mathematical Institute (LOMI)*, preprint P-6-89, Leningrad, (in Russian).

Banichuk, N.V., 1970, "Determination of the Form of a Curvilinear Crack by Small Parameter Technique," *Izv. An SSR, MTT 7*, Vol. 2, pp. 130–137 (in Russian).

Claussen, N., 1976, "Fracture toughness of Al_2O_3 with an unstabilized ZrO_2 dispersed phase," *J. Am. Ceram. Soc.*, Vol. 59, pp. 49–51.

Cotterell, B., and Rice, J.R., 1980, "Slightly curved or kinked cracks," *Int. Journal of Fracture*, Vol. 16, No. 2, pp. 155–169.

Duan, K., Mai, Y.W., and Cotterel, B., 1976, "On the paradox between crack bridging and crack interaction in quasi-brittle materials," *J. Europ. Ceram. Soc.*, Vol. 15, pp. 1061–1064.

Fichera, G., 1972, "Unilateral constraints in elasticity," *Handbuch der Physik*, Vol. VI a/2, S. Flügge, ed., Springer-Verlag, Berlin.

Goldstein, R.V., and Salganik, R.L., 1974, "Brittle fracture of solids with arbitrary cracks," *Int. J. Fracture*, Vol. 10, pp. 507–523.

Movchan, A.B., 1992, "Integral characteristics of elastic inclusions and cavities in the two-dimensional theory of elasticity," *Eur. J. Appl. Math.*, Vol. 3, pp. 21–30.

Movchan, A.B., Nazarov, S.A., and Polyakova, O.R., 1991, "The quasi-static growth of a semi-infinite crack in a plane containing small defects," *Comptes Rendus de L'Academie des Sciences. Paris, Série II*, Vol. 313, pp. 1223–1228.

Movchan, A.B., and Movchan, N.V., 1995, *Mathematical modelling of solids with non regular boundaries*, CRC Press, Boca Raton, FL.

Movchan, A.B., and Serkov, S.K., 1991, "Elastic polarisation matrices for polygonal domains," *Mech. Solids*, Vol. 26, No. 3, pp. 63–68.

Muskhelishvili, N.I., 1953, *Some basic problems of the mathematical theory of elasticity*, Noordhoff, Groningen.

Pólya, G., and Szegö, G., 1951, *Isoperimetric inequalities in mathematical physics*, Princeton, University Press, Princeton, NJ.

Rose, L.R.F., 1986, "Microcrack interaction with a main crack," *Int. J. Fracture*, Vol. 31, pp. 233–242.

Rubinstein, A.A., 1986, "Macro-crack—Micro-defect Interaction," ASME JOURNAL OF APPLIED MECHANICS, Vol. 53, pp. 505–510.

Zorin, I.S., Movchan, A.B., and Nazarov, S.A., 1988, "The use of the elastic polarisation tensor in problems of crack mechanics," *USSR Izvestiya Mechanics of Solids*, Vol. 26, No. 6, pp. 128–134 (in Russian).